Materials Transactions, Vol. 46, No. 7 (2005) pp. 1720 to 1724

EXPRESS REGULAR ARTICLE

New Pd-Based Bulk Glassy Alloys with High Glass-Forming Ability and Large Supercooled Liquid Region

Kana Takenaka[1], Takeshi Wada[1], Nobuyuki Nishiyama[2], Hisamichi Kimura[3] and Akihisa Inoue[3]

[1]*Graduate School, Tohoku University, Sendai 980-8577, Japan*
[2]*RIMCOF Tohoku Univ. Lab., R&D Institute of Metals and Composites for Future Industries, Sendai 980-8577, Japan*
[3]*Institute for Materials Research, Tohoku University, Sendai 980-8577, Japan*

With the aim of developing a new bulk glassy alloy which can be applied to biomedical applications, we examined glass-forming ability and mechanical properties of Ni-free glassy alloys in $Pd_{50-x}Pt_xCu_{30}P_{20}$ system. As a result, the best glass-forming composition is located at $Pd_{35}Pt_{15}Cu_{30}P_{20}$, and the alloy can be formed into bulk glassy rods with diameters of up to at least 30 mm by fluxed water quenching. For the bulk glassy alloy, fracture strength, fracture elongation and Young's modulus were measured to be 1590 MPa, 1.8% and 99.8 GPa, respectively, under a compressive stress and 1410 MPa, 1.7% and 83.0 GPa, respectively, under a tensile stress. These features of high glass-forming ability and good mechanical properties are expected to be used as biomedical materials.

(Received April 4, 2005; Accepted May 18, 2005; Published July 15, 2005)

Keywords: *biomedical application, Ni-allergy, high strength, low Young's modulus*

1. Introduction

Recent years, bulk glassy alloys have attracted much attention because of their useful characteristics which are significantly different from those of crystalline alloys in a bulk material form.[1–4)] Motivation of the recent attention to bulk glassy alloys has been attributed to the syntheses of Mg-,[5)] La-[6)] and Zr-[7)] based bulk glassy alloys consisting only of metallic elements for several years between 1988 and 1990, though glassy alloy rods up to 2 mm and glassy alloy spheres with diameters up to 9 mm in Pd–Ni–P system were produced by water quenching[8)] and many repeated melting together with B_2O_3 flux medium, respectively.[9)] Focusing on Pd-based bulk glassy alloys, the Pd–Ni–P alloy component was found in 1969.[10)] The maximum diameter of the Pd–Ni–P ternary glassy alloys in the case of conventional copper mold casting or water quenching is about 2 mm.[8)] It has been found in 1996 that the replacement of Ni by 30 at% Cu in $Pd_{40}Ni_{40}P_{20}$ alloy causes a drastic increase in the maximum diameter to more than 40 mm even in a non-fluxed melting state.[11)] Very recently, Pd- and Pt-based bulk glassy alloys have drawn increasing interest as biomedical materials. In their application field, it is necessary to develop a Pd-based bulk glassy alloy without Ni element. The complete elimination of Ni element in Pd-based alloys has been recognized to significantly decrease the glass-forming ability as well as the supercooled liquid region before crystallization.[12)] For instance, the maximum sample diameter and the temperature interval of supercooled liquid region are about 100 mm and 95 K, respectively, for $Pd_{40}Cu_{30}Ni_{10}P_{20}$[13)] and less than 1 mm and 48 K, respectively, for $Pd_{40}Cu_{40}P_{20}$.[12)] We have found that the partial replacement of Pd by Pt in $Pd_{40}Cu_{40}P_{20}$ alloy is effective for the increases in maximum sample diameter and supercooled liquid region and the resulting Pd–Pt–Cu–P bulk glassy alloy can be regarded as a new type of Pd-based bulk glassy alloy which is important for basic research and biomedical application. This paper presents the glass-forming ability, thermal stability and mechanical properties of the new Pd–Pt–Cu–P bulk glassy alloys and to investigate the reason for the effectiveness of Pt addition on the glass-forming ability and thermal stability of supercooled liquid against crystallization.

2. Experimental Procedures

Ternary and quaternary Pd-based alloy ingots with composition of $Pd_{50-x}Pt_xCu_{30}P_{20}$ ($x = 0$ to 20 at%) were prepared by induction melting pure Pd, Pt and Cu metals, pre-sintered Pd–P and Pt–P alloys in an argon atmosphere. The alloy compositions represent nominal atomic percentages. Bulk glassy alloy rods with diameters up to 30 mm were prepared by copper mold casting and water quenching methods. Glassy alloy ribbons with a cross section of $0.025 \times 1.2\,mm^2$ were also produced by the melt spinning method. Glassy structure was examined by X-ray diffraction. Thermal stability associated with glass transition (T_g), crystallization temperature (T_x) and supercooled liquid region ($\Delta T_x = T_x - T_g$), as well as melting (T_m) and liquidus temperatures (T_l) was examined by differential scanning calorimetry (DSC) at a heating rate of 0.67 K/s. Mechanical strength was examined using an Instron testing machine. For the compressive test, the machined samples with a diameter of 3 mm and a length of 6 mm were used at a strain rate of $1.0 \times 10^{-4}\,s^{-1}$. For the tensile test, the dog-bone-shaped samples with a gauge diameter of 2 mm and a gauge length of 10 mm were used at a strain rate of $5.0 \times 10^{-4}\,s^{-1}$. Fracture surface of the test samples was examined by scanning electron microscopy (SEM).

3. Results and Discussion

A glassy single phase in the $Pd_{50-x}Pt_xCu_{30}P_{20}$ alloys was formed in the composition range of 0 to 20 at% Pt by the melt-spinning and water quenching. Figure 1 shows DSC curves of the melt-spun glassy $Pd_{50-x}Pt_xCu_{30}P_{20}$ alloys. All the samples exhibit an endothermic reaction due to glass transition, followed by a supercooled liquid region and then a sharp exothermic peak due to crystallization, revealing the

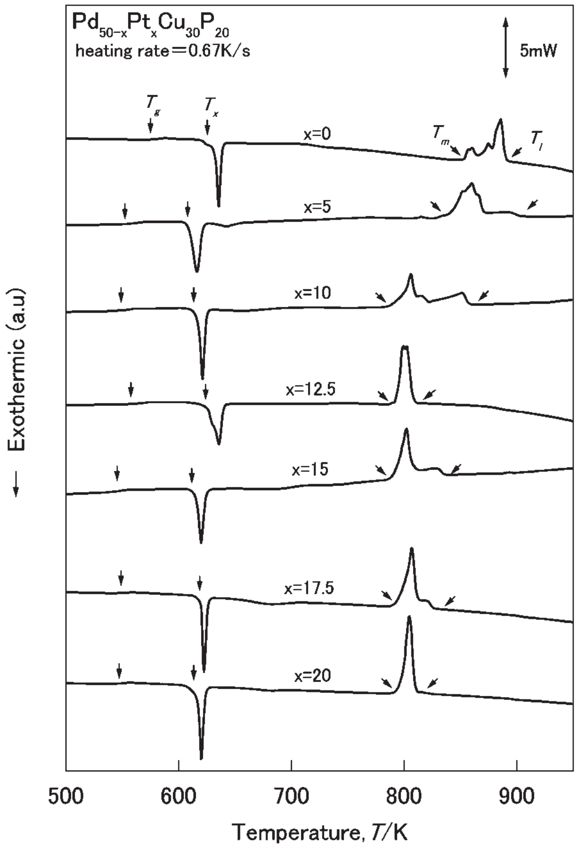

Fig. 1 Differential scanning calorimetric (DSC) curves of melt-spun $Pd_{50-x}Pt_xCu_{30}P_{20}$ glassy alloys.

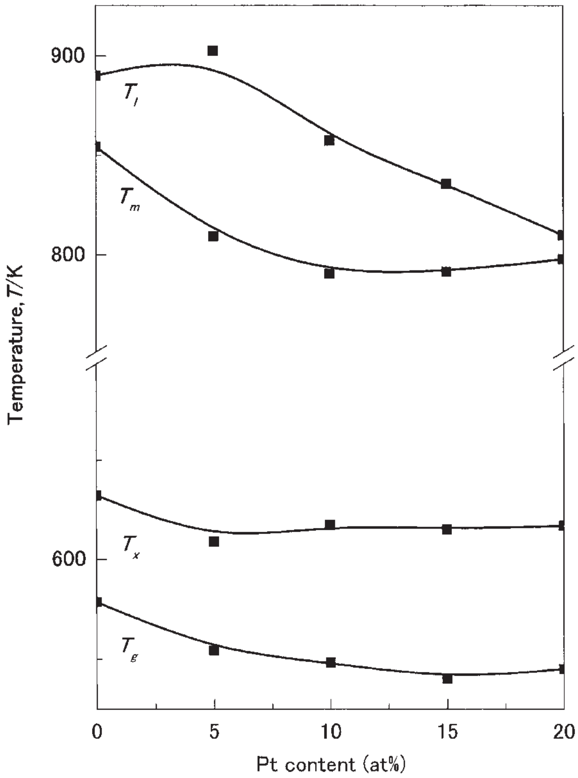

Fig. 2 Glass transition temperature (T_g), crystallization temperature (T_x), melting temperature (T_m), and liquidus temperature (T_l) as a function of Pt content for $Pd_{50-x}Pt_xCu_{30}P_{20}$ glassy alloys.

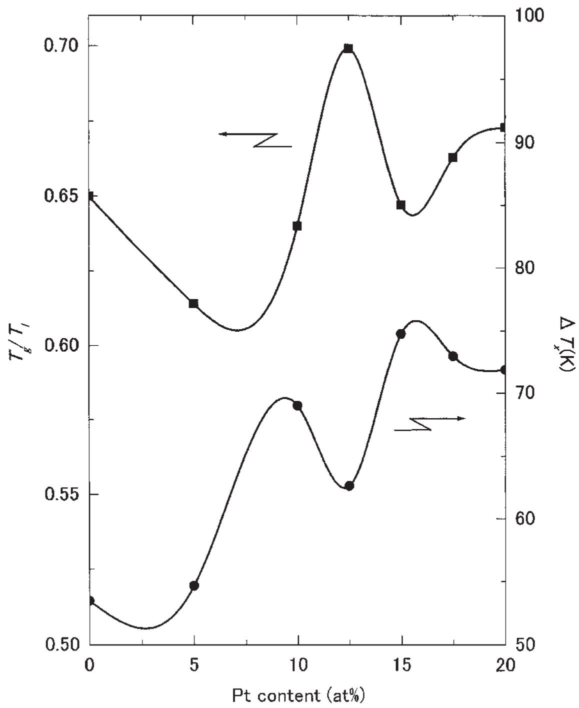

Fig. 3 Supercooled liquid region ($\Delta T_x = T_x - T_g$) and reduced glass transition temperature (T_g/T_l) as a function of Pt content for Pd_{50-x}-$Pt_xCu_{30}P_{20}$ glassy alloys.

thermal characteristics typical for glassy structure. With further increasing temperature, several steps of endothermic peaks due to melting can be observed. These characteristic temperatures such as T_g, T_x, T_m and T_l as a function of Pt content for the $Pd_{50-x}Pt_xCu_{30}P_{20}$ alloys are summarized in Fig. 2. T_x is almost constant in the Pt content range above 5 at%, while T_g slightly decreases with increasing Pt content, leading to an increase in ΔT_x. On the other hand, T_m and T_l decrease with increasing Pt content. It is therefore interpreted that the Pt addition leading to the decrease on T_l and the increase in ΔT_x is effective for the enhancement of glass-forming ability.

In order to estimate their glass-forming ability, ΔT_x and reduced glass transition temperature (T_g/T_l) derived from the characteristic temperatures are shown in Fig. 3. Both ΔT_x and T_g/T_l values are recognized as quantitative parameters revealing glass-forming ability. As shown in the figure, the changes in ΔT_x and T_g/T_l values with Pt content are complicated. However, there is a clear tendency for ΔT_x to increase with increasing Pt content, show a maximum value of 75 K at $x = 15$ at%, and then decrease in the higher Pt content range. On the other hand, T_g/T_l shows the similar behavior as that for ΔT_x, though the maximum value of 0.70 is obtained at the different content of 12.5 at% Pt. This difference in the optimum Pt contents between the parameters reflects the difference in characters for each parameter. That is, ΔT_x and T_g/T_l reflect the resistance for crystallization from supercooled liquid state and kinetic stability of undercooled melt, respectively.[14] These results suggest that the best glass-forming composition lies in the vicinity of $Pd_{35}Pt_{15}Cu_{30}P_{20}$. To confirm the best glass-forming composition, the critical diameter for formation of a single glassy

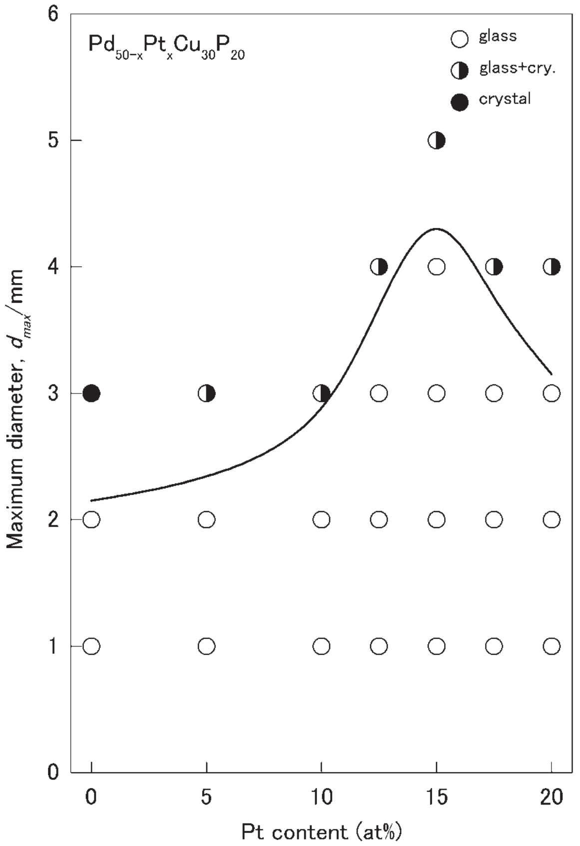

Fig. 4 Maximum rod diameter (d_{max}) as a function of Pt content for $Pd_{50-x}Pt_xCu_{30}P_{20}$ glassy alloys produced by copper mold casting.

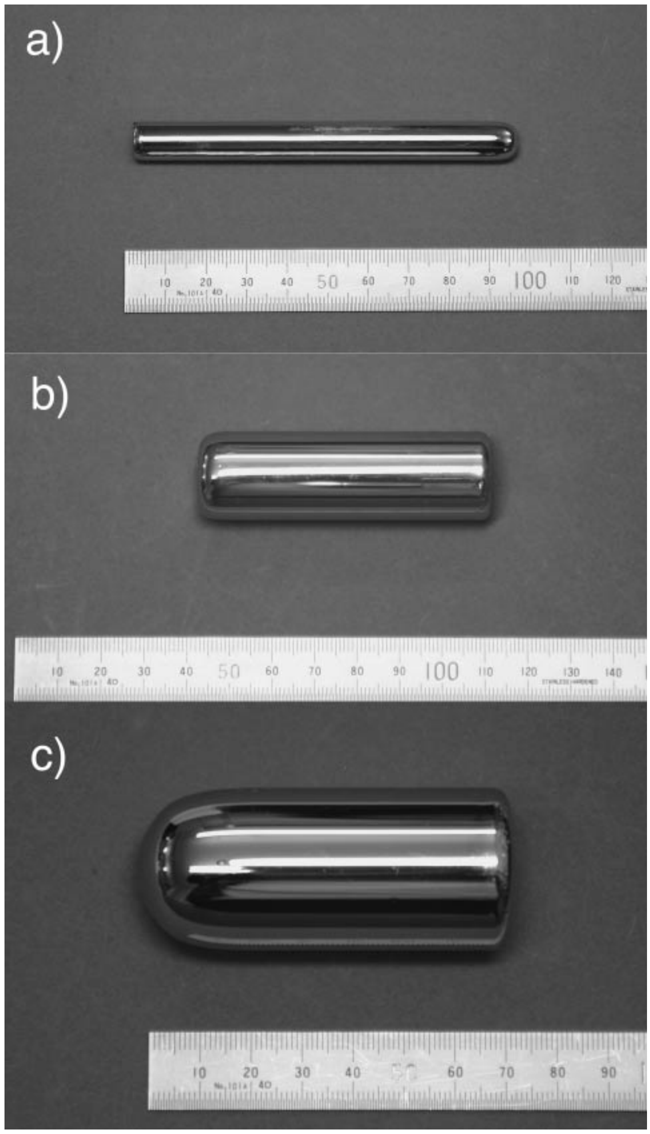

Fig. 5 Outer shape of $Pd_{35}Pt_{15}Cu_{30}P_{20}$ glassy alloy rods with diameters of 10, 20 and 30 mm produced by water quenching.

phase (d_{max}) was investigated for the bulk alloys produced by copper mold casting. Figure 4 shows the d_{max} as a function of Pt content. It is clear that the maximum value of d_{max} is 4 mm at $x = 15$ at%, and this behavior is consistent with the change in ΔT_x value. As seen in Fig. 2, the T_m changes with Pt content, suggesting that the alloys with Pt contents of 0 to 20 at% do not lie within the same eutectic valley. In such a situation, the ΔT_x value may be preferable to represent the glass-forming ability. It is thus concluded that the best alloy composition for glass-formation is $Pd_{35}Pt_{15}Cu_{30}P_{20}$ and its d_{max} value is 4 mm in the case of copper mold casting method.

Glass-forming ability of Pd- and Pt-based alloys often degrades due to impurity which causes heterogeneous nucleation during copper mold casting.[15] To clarify the ultimate glass-forming ability of the $Pd_{35}Pt_{15}Cu_{30}P_{20}$ alloy, large-sized samples are prepared employing B_2O_3 flux treatment by the water quenching method. Figure 5 shows the outer shape and surface appearance of $Pd_{35}Pt_{15}Cu_{30}P_{20}$ glassy alloy rods with diameters of (a) 10, (b) 20 and (c) 30 mm produced by water quenching. All the rod samples are very smooth and exhibit good luster. To compare the thermal stability, DSC curves of $Pd_{35}Pt_{15}Cu_{30}P_{20}$ alloy rods with different diameters are shown in Fig. 6, together with the data of the melt-spun glassy ribbon. Although the cooling rates of the rod samples are several orders of magnitude smaller than that of the ribbon sample, no distinct difference in the thermal characteristic temperatures is recognized. This result suggests that the $Pd_{35}Pt_{15}Cu_{30}P_{20}$ alloy possesses extremely high glass-forming ability and the ultimate d_{max} is at least 30 mm or more under the well-fluxed condition. It is worthy to note that the $Pd_{35}Pt_{15}Cu_{30}P_{20}$ alloy has the highest glass-forming ability among the glass-forming system without Ni content, so far.

In a biomedical application, mechanical properties as well as glass-forming ability are important. Figure 7 shows the stress–strain curves of the $Pd_{35}Pt_{15}Cu_{30}P_{20}$ bulk glassy alloy under compressive and tensile applied stresses. Under a compressive stress, the rod sample shows a typical deformation behavior of glassy alloy, *i.e.*, high elastic deformation limit with low Young's modulus, and then catastrophic fracture at high fracture strength. Fracture strength, fracture strain and Young's modulus of the alloy under a compressive applied stress are evaluated to be 1590 MPa, 0.018 and 99.8 GPa, respectively. These mechanical properties are good enough to be applied for biomedical uses. Furthermore, almost the same properties are obtained even under a tensile applied stress. Fracture strength, fracture strain and Young's modulus of the alloy under a tensile stress are evaluated to be

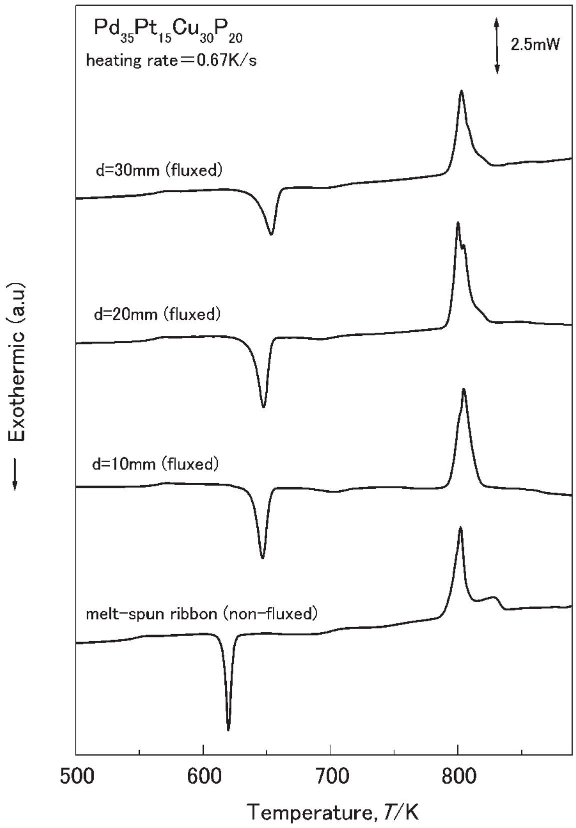

Fig. 6 DSC curves of $Pd_{35}Pt_{15}Cu_{30}P_{20}$ bulk glassy alloy rods with different diameters. The data of the ribbon sample are also shown for comparison.

1410 MPa, 0.017 and 83.0 GPa, respectively. This coincidence in fracture strength between compressive and tensile applied stress conditions indicates that the alloy can retain good mechanical properties not only under an actual three-dimensional stress but also under a more severe uni-axial tensile stress. The good mechanical properties are attributed to the synergetic effects of homogeneous structure due to the extremely high glass-forming ability and inclusion-free quality due to the complete flux treatment.

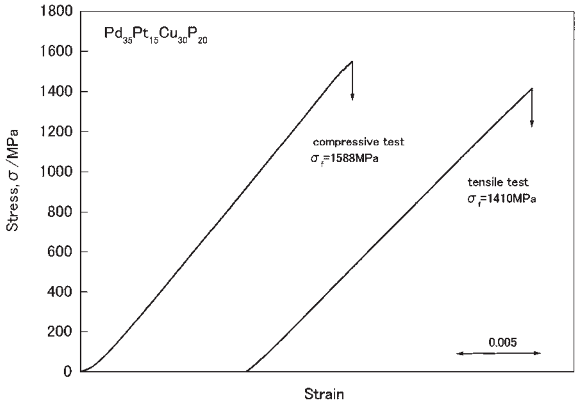

Fig. 7 Stress–strain curves of the $Pd_{35}Pt_{15}Cu_{30}P_{20}$ glassy alloy rods under compressive and tensile loads.

Figure 8(a) shows a SEM image of the $Pd_{35}Pt_{15}Cu_{30}P_{20}$ glassy alloy rod subjected to the fracture under compressive load. The catastrophic fracture occurred along a maximum shear stress plane, which was inclined by about 45 degrees to the direction of the applied load. A well-developed vein-pattern can be seen on the fracture surface, indicating good ductile nature of the alloy. On the other hand, a more complicated fracture behavior under tensile stress in comparison with that under compressive stress can be seen in Fig. 8(b). That is, a shear slip initially might occur on the left hand side region of the fracture surface along with about 45 degrees to the direction of the applied tensile load, and then, the stress mode suddenly changes from uni-axial shear slip (mode II) to bi-axial opening (mode I). This change in stress mode appears to cause the morphology change in the right hand side region of the fracture surface. The slightly lower tensile strength of 1410 MPa as compared with the compressive strength of 1590 MPa is attributed to the mode change of the applied stress. However, the well-developed vein pattern is observed even on the right side of the fracture surface. These vein-patterns appeared both on the compressive and tensile fracture surfaces are regarded as the evidence of

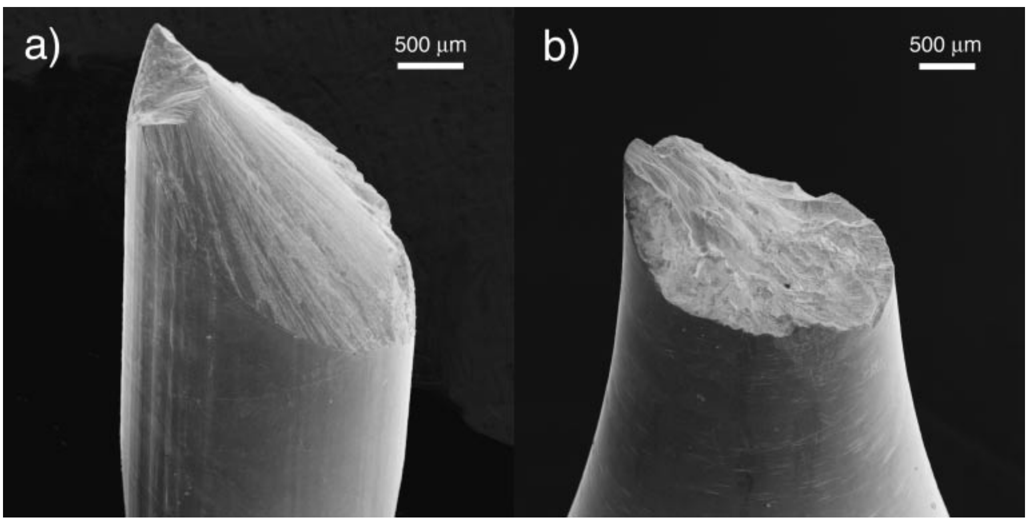

Fig. 8 Scanning electron micrographs of the fracture appearance of the $Pd_{35}Pt_{15}Cu_{30}P_{20}$ glassy alloy rod subjected to a) compressive and b) tensile fractures.

Table 1 Thermal stability and mechanical properties of some Pd-based bulk glassy alloys in Pd–Ni–P, Pd–Cu–Ni–P and Pd–Pt–Cu–P systems.

	T_g (K)	T_x (K)	ΔT_x (K)	σ_f (MPa)	ε_f	H_v
$Pd_{40}Ni_{40}P_{20}$	589[16]	670[16]	81[16]	1400[17]	1.65[17]	538 ± 16[18]
$Pd_{40}Cu_{30}Ni_{10}P_{20}$[12]	575	670	95	1640	1.80	515 ± 30
$Pd_{35}Pt_{15}Cu_{30}P_{20}$	540	615	75	1410	1.74	470 ± 15

ductile nature of the glassy alloy. Furthermore, the high strength property exceeding 1400 MPa under the tensile stress mode is the proof that the new Pd-based bulk glassy alloy possesses good mechanical properties.

Table 1 summarizes the thermal characteristic temperatures, mechanical properties and d_{max} for the Pd–Ni–P[16–18] ternary, the Pd–Cu–Ni–P[12] quaternary and the present Pd–Pt–Cu–P alloys. The d_{max} of the Pd–Pt–Cu–P alloy exceeds that of the ternary alloy. Therefore the replacement of Pd by Pt is effective to enhance the glass-forming ability of the ternary alloy, and its glass-forming ability is comparable to that for the Pd–Cu–Ni–P alloy which is the easiest glass-former, so far. In addition, the thermal stability and mechanical properties are quite similar among the three glass-forming alloys. It is important to note that the present Pd–Pt–Cu–P alloy exhibits mostly high glass-forming ability, high thermal stability and good mechanical properties in absence of Ni element. These futures will be applicable for biomedical application.

4. Conclusions

A new glassy Pd–Pt–Cu–P alloy without Ni element has been synthesized for biomedical application. The best glass-forming composition is found to be $Pd_{35}Pt_{15}Cu_{30}P_{20}$ and the alloy can be formed into bulk glassy rods with diameters of 4 and 30 mm by copper mold casting and fluxed water quenching, respectively. Fracture strength, fracture elongation and Young's modulus of the glassy alloy are evaluated to be 1590 MPa, 1.8% and 99.8 GPa, respectively, under a compressive stress and 1410 MPa, 1.7% and 83.0 GPa, respectively, under a tensile stress. These features of high glass-forming ability, high thermal stability and good mechanical properties are expected to be used as biomedical materials.

REFERENCES

1) A. Inoue: Mater. Trans., JIM **36** (1995) 866–875.
2) A. Inoue: Acta Mater. **48** (2000) 279–306.
3) A. Inoue: Mater. Sci. Eng. A **304–306** (2001) 1–10.
4) Supercooled Liquid Bulk Glassy and Nanocrystalline State of Alloys, ed. by A. Inoue, A. R. Yavari, W. L. Johnson and R. H. Dauskardt, (MRS, warrendale, 2001) pp. L12.13.1–L12.13.6.
5) A. Inoue, A. Kato, T. Zhang, S. G. Kim and T. Masumoto: Mater. Trans., JIM **32** (1991) 609–616.
6) A. Inoue, T. Zhang and T. Masumoto: Mater. Trans., JIM **30** (1989) 965–972.
7) A. Inoue, T. Zhang and T. Masumoto: Mater. Trans., JIM **31** (1991) 1005–1010.
8) A. J. Drehman, A. L. Greer and D. Turnbull: Appl. Phys. Lett. **41** (1982) 716–717.
9) H. W. Kui, A. L. Greer and D. Turnbull: Appl. Phys. Lett. **45** (1984) 615–616.
10) H. S. Chen and D. Turnbull: Acta Metall. **17** (1969) 1021–1031.
11) A. Inoue, N. Nishiyama and T. Matsuda: Mater. Trans., JIM **37** (1996) 181–184.
12) N. Nishiyama: Dr Thesis 1997, Tohoku university.
13) A. Inoue, N. Nishiyama and H. M. Kimura: Mater. Trans., JIM **38** (1997) 179–183.
14) N. Nishiyama and A. Inoue: Mater. Trans. **43** (2002) 1913–1917.
15) Supercooled Liquid Bulk Glassy and Nanocrystalline State of Alloys, ed. by A. Inoue, A. R. Yavari, W. L. Johnson and R. H. Dauskardt, (MRS, warrendale, 2001) pp. L3.1.1.
16) J. P. Chu, C. L. Chiang, T. G. Nieh and Y. Kawamura: Intermetallics **10** (2002) 1191–1195.
17) Y. Zheng, T. Wada, N. Nishiyama and A. Inoue: unpublished research.
18) U. Ramamurty, S. Jana, Y. Kawamura and K. Chattopadgyay: Acta Mater. **53** (2005) 705–717.